

## A single-stage AC conversion with the three-phase matrix converter for the constant V/f ratio method

Prasopchok Hothongkham<sup>1</sup>, Sataporn Suathed<sup>2</sup>, Anuchit Aurairat<sup>3</sup>

<sup>1</sup>Department of Electrical Engineering, Faculty of Engineering, Rajamangala University of Technology, Rattanakosin, Thailand

<sup>2</sup>Department of Mechatronics Engineering, Faculty of Engineering, Rajamangala University of Technology, Rattanakosin, Thailand

<sup>3</sup>Department of Electrical Engineering Technology, Faculty of Industrial and Technology,  
Rajamangala University of Technology, Rattanakosin, Thailand

### Article Info

#### Article history:

Received Sep 29, 2024

Revised Jan 27, 2025

Accepted Mar 29, 2025

#### Keywords:

AC to AC converter

Direct AC-AC converter

Matrix converter

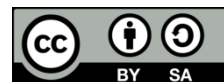
PWM converter

PWM generation

### ABSTRACT

This research introduces a single-stage direct three-phase matrix converter that utilizes the signals from the output voltage for designing pulse-width modulation signals. This converter is made up of nine bidirectional switches that use IGBT power diodes. It directly converts a steady three-phase source voltage and frequency into a variable output voltage and frequency by adjusting the frequency and modulation index of the pulse-width modulation (PWM) signals. A mathematical model is utilized to illustrate the basic principles of the matrix converter before examining its operational waveform. An evaluation is then made between the analytical waveforms and the functional waveforms, as well as the harmonics generated by the direct three-phase matrix converter. The results from both methods and processes are displayed in close agreement. Additionally, this paper discusses V/f control for induction motor drive control using this converter.

This is an open access article under the [CC BY-SA](#) license.



### Corresponding Author:

Sataporn Suathed

Department of Mechatronics Engineering, Faculty of Engineering, Rajamangala University of Technology  
Rattanakosin, Thailand

Email: sataporn.sua@rmutr.ac.th

## 1. INTRODUCTION

The matrix converter (MC) was primarily introduced by Gyugyi and Pelly in 1971 and 1976 [1], [2]. By 1980, the concept was further developed into a mathematical model by Alesina and Venturini [3], as well as Ziogas *et al.* [4]. The objective of using the MC was to eliminate the DC link, typically crucial in inverter circuits. These ideas were further explored by Alesina and Venturini [5], also Ziogas *et al.* [6]. Lately, the three-phase matrix converter has attracted considerable interest for its lack of a DC link capacitor and its capability to regulate bidirectional power flow. Applications of the matrix converter in telecommunication systems are discussed in [7], highlighting its advantage of omitting a capacitor in the circuit and its impact on power flow. Simulation using MATLAB/Simulink, presented in [8], demonstrated SVM algorithms for passive loads. The Venturini method was selected to control and evaluate the performance of the apparatus. The matrix converter was regulated to provide a three-phase output with adjustable voltage and frequency [9]. The result [10] presents four algorithms for the three-phase matrix converter using MATLAB/Simulink, comparing harmonic distortion in voltages and currents. Additionally, Heris *et al.* [11] introduced the three-phase cyclo-converter using PSCAD/EMTDC software for load testing, demonstrating the effectiveness and achievements of the proposed circuit. A pulse-width modulation (PWM) method for a matrix converter circuit with a three-phase source input and five-phase variable output voltage and frequency is proposed [12].

The sophisticated pulse-width modulation control method is founded on the space vector principle. Another work proposes an indirect matrix converter (IMC) circuit with dual three-phase outputs and a carrier-

based pulse-width modulation method that provides dual three-phase supplies for two three-phase loads [13]. A space vector control principle has been designed for a three-to-seven-phase matrix converter, enabling the direct conversion of a three-phase input voltage and frequency into a seven-phase output with variable voltage and frequency [14]. The three-phase neutral point clamped (NPC) matrix converter structure is developed using space vector modulation without Park transformation [15]. Furthermore, FPGA technology is applied for PLL synchronization and SVPWM modulation, abbreviating the dependence on microcontrollers and parallelizing the process [16]. Carrier-based space vector modulation for matrix converters, utilizing indirect transfer function access, is used for controlling the matrix converter, as presented in [17]. The three-phase phase-modular isolated indirect matrix-type Y/ $\Delta$  PFC rectifier (IM Y/D rectifier) is analyzed and operated with the ZVS technique to minimize overall losses in a SiC MOSFET-based prototype rectifier [18]. The pulse-width modulation control of a three-phase matrix converter, achieving lower voltage harmonics and the target output voltage, is demonstrated by selecting appropriate switching patterns and generating duty cycles using the MATLAB/Simulink program [19]. The topology of a three-phase matrix converter without DC energy storage for power flow control and compensation of deep voltage sags and swells is presented in [20].

Shinde and Date [21] discuss the direct three-phase AC-AC matrix converter with bidirectional power control for inductive power transfer (IPT) systems, including controller design techniques, simulation analysis, and experimental results for an inductive battery charging system. A new six-phase to three-phase multilevel matrix converter (6 $\times$ 3 MMC) principle is suggested in [22], featuring two series-connected current source rectifiers (CSRs) on the input side and a three-level T-type inverter on the output side, using a carrier-based pulse-width modulation (CB pulse-width modulation) technique. Modulation strategies based on mathematical construction for a three-to-five-phase matrix converter (3 $\times$ 5 MC) are presented, offering reduced computational complexity compared to traditional space vector modulation, with verification through simulations [23]. The pulse-width modulation signals in a bidirectional isolated AC-DC matrix converter (BIMC) can adjust the phase shift angle and pulse width for both the front-stage matrix circuit and the back-stage full-bridge circuit. The power factor is close to unity, and the load dynamic response is fast, as shown in simulation results [24]. A three-phase to single-phase direct matrix converter is demonstrated, showing output voltage frequency variation with switching frequency changes in pulse-width modulation signals through simulation [25]. Additionally, a three-phase matrix converter (MC) for wireless power transfer (WPT) is proposed, with an improved modulation strategy to reduce total harmonic distortion (THD) of the supply current in both resonant and non-resonant states. The practicality and effectiveness of the proposed modulation strategy are confirmed by experiments [26].

The high-frequency link three-phase (HFLTP) AC-DC converter consists of a matrix converter on the AC side and a full-bridge converter interconnected via a high-frequency transformer to the loads, utilizing the SVPWM technique for soft-switching and soft commutation, with clear results [27]. In the previously mentioned articles, signal comparisons were used for PWM generation to control the switches. This paper focuses on PWM generation using output voltage signals to control the bidirectional switches in a three-phase matrix converter circuit. The number of the output voltage pulses can be determined by  $3n$  ( $n = 1, 2, 3, \dots$ ). This method can effectively reduce the harmonic output voltage by increasing the number of pulses. The harmonic orders can be determined by the lower and higher harmonic orders, as well as their reduction with the number of pulses. This study emphasizes the concept of the 6-pulse three-phase matrix converter using mathematical equations and its implementation through theoretical waveforms. It allows for varying output frequencies and voltages by modifying both the frequency and modulation index of the pulse-width modulation signals, providing useful reference data for various applications, including V/f control of induction motor drives. Moreover, these bi-directional switches are easy to control, making them suitable for direct conversion and various applications. On the contrary, the switching losses in these switches are a disadvantage.

## 2. THE THREE-PHASE PULSE-WIDTH MODULATION MATRIX CONVERTER PRINCIPLE

The three-phase PWM matrix converter is illustrated in Figure 1. It is possible to describe the three-phase PWM matrix converter using mathematical equations before its implementation takes place. This can be done through practical and theoretical waveforms as outlined below:

### 2.1. A theoretical analysis of the three-phase pulse-width modulation matrix converter [28]-[30]

Figure 1 illustrates the topology of the three-phase pulse-width modulation matrix converter, which can transform a fixed 3-phase utility into a desirable output voltage and frequency. The Pulse-width modulation signals can be adjusted to modify the frequency, voltage, and number of pulses, thereby controlling the output voltage. Additionally, the output voltage of this converter can be adjusted by modifying the voltage, frequency, and number of pulses using pulse-width modulation signals. Consequently, this converter can be utilized within a six-port configuration, consisting of 3 pairs of input and output ports. Additionally, the matrix converter (MC)

is able to be viewed as three independent 3-phase to 1-phase cyclo-converters. The mathematical model for the distinct MC is provided as part of (1) through (6).

$$[V_{oAB}(\omega_o t)] = [V_i \cos(\omega_i t), V_i \cos(\omega_i t - 120^\circ), V_i \cos(\omega_i t + 120^\circ)] \times \begin{bmatrix} M \cos(\omega_i t) \\ M \cos(\omega_i t - 120^\circ) \\ M \cos(\omega_i t + 120^\circ) \end{bmatrix} \times [\cos(\omega_o t)] \quad (1)$$

$$= \begin{bmatrix} MV_i \cos(\omega_i t) \cos(\omega_i t) \\ MV_i \cos(\omega_i t - 120^\circ) \cos(\omega_i t - 120^\circ) \\ MV_i \cos(\omega_i t + 120^\circ) \cos(\omega_i t + 120^\circ) \end{bmatrix} \times [\cos(\omega_o t)] \quad (2)$$

$$= \frac{MV_i}{2} [\cos(2\omega_i t) + \cos(0^\circ) + \cos(2\omega_i t - 240^\circ) + \cos(0^\circ) + \cos(2\omega_i t + 240^\circ) + \cos(0^\circ)] \times \cos(\omega_o t) \quad (3)$$

$$= \left[ \frac{3MV_i}{2} \right] \times [\cos(\omega_o t)] \quad (4)$$

$$[V_{oBC}(\omega_o t)] = \left[ \frac{3MV_i}{2} \right] \times [\cos(\omega_o t - 120^\circ)] \quad (5)$$

$$[V_{oCA}(\omega_o t)] = \left[ \frac{3MV_i}{2} \right] \times [\cos(\omega_o t + 120^\circ)] \quad (6)$$

$$\begin{bmatrix} V_{oAB}(\omega_o t) \\ V_{oBC}(\omega_o t) \\ V_{oCA}(\omega_o t) \end{bmatrix} = \left[ \frac{3MV_i}{2} \right] \times \begin{bmatrix} \cos(\omega_o t) \\ \cos(\omega_o t - 120^\circ) \\ \cos(\omega_o t + 120^\circ) \end{bmatrix} \quad (7)$$

Where,  $V_{oAB}$ ,  $V_{oBC}$ ,  $V_{oCA}$  are the line output voltages.  $M$  is the modulation indexes.  $V_i$  are the input voltages.

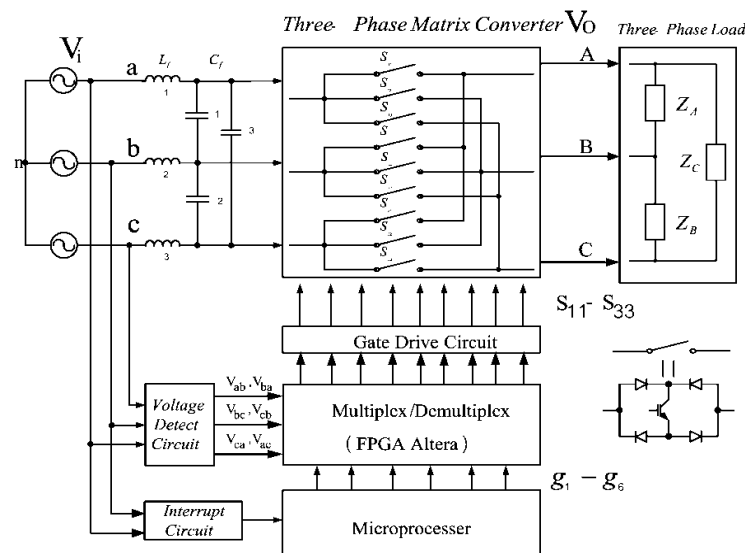


Figure 1. The three-phase pulse-width modulation matrix converter showing the proposed power circuit

In Figure 2 presents the equations in graphical format, including the waveforms of (1) through (7). Figure 2(a) shows the input voltages  $V_{iab}$ ,  $V_{ibc}$ , and  $V_{ica}$ , while Figures 2(b) through 2(d) depict the corresponding switching functions  $M \cos(\omega_i t)$ ,  $M \cos(\omega_i t - 120^\circ)$ , and  $M \cos(\omega_i t + 120^\circ)$ . Figure 2(e) illustrates the term  $MV_i \cos(\omega_i t) \cos(\omega_i t)$ , which represents the result derived from the input voltage  $V_{iab}$

demonstrated by Figure 2(a) and the switching function presented by Figure 2(b). Figure 2(f) displays the term  $MV_i \cos(\omega_i t - 120^\circ) \cos(\omega_i t - 120^\circ)$ , and Figure 2(g) shows the term  $MV_i \cos(\omega_i t + 120^\circ) \cos(\omega_i t + 120^\circ)$ . The waveforms depicted in Figures 2(e)-2(g) are able to be combined to form (8). The resulting waveform, a 6-pulse full-wave, is shown in Figure 2(h). This switching function is used to multiply the full-wave result depicted in Figure 2(i). Figure 2(j) displays the simulation results, while Figure 2(k) presents the experimental results.

$$\begin{aligned} & \left[ \frac{MV_i}{2} (\cos(2\omega_i t) + \cos(0^\circ)) \right] \\ & + \left[ \frac{MV_i}{2} (\cos(2\omega_i t - 240^\circ) + \cos(0^\circ)) \right] \\ & + \left[ \frac{MV_i}{2} (\cos(2\omega_i t + 240^\circ) + \cos(0^\circ)) \right] \end{aligned} \quad (8)$$

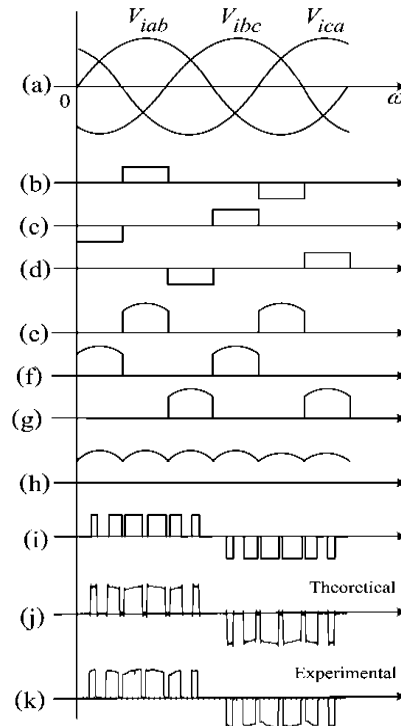


Figure 2. The theoretical and practical waveforms obtained from the mathematical equations: (a) three-phase waveforms, (b) switching functions  $M \cos(\omega_i t)$ , (c) switching functions  $M \cos(\omega_i t - 120^\circ)$ , (d) switching functions  $M \cos(\omega_i t + 120^\circ)$ , (e) two-pulse full-wave  $MV_i \cos(\omega_i t) \cos(\omega_i t)$ , (f) two-pulses full-wave  $MV_i \cos(\omega_i t - 120^\circ) \cos(\omega_i t - 120^\circ)$ , (g) two-pulses full-wave  $MV_i \cos(\omega_i t + 120^\circ) \cos(\omega_i t + 120^\circ)$ , (h) six-pulses full-wave, (i) PWM Switching functions, (j) output waveform  $V_{OAB}$  from theory, and (k) output waveform  $V_{OAB}$  from experiment

## 2.2. A practical of the three-phase pulse-width modulation matrix converter

Figure 1 presents the power circuit of the matrix converter (MC), which includes 9 bi-directional switches controlled by pulse-width modulation signals  $S_{11} - S_{33}$ . The PWM signals are derived from the pulse-width modulation signals  $g_1 - g_6$  and these signals for control as  $V_{ab}$ ,  $V_{ac}$ ,  $V_{bc}$ ,  $V_{ba}$ ,  $V_{ca}$ , and  $V_{cb}$  via a multiplexer/demultiplexer circuit. The microprocessor generates the pulse-width modulation signals  $g_1 - g_6$ , while the signals for control as  $V_{ab}$ ,  $V_{ac}$ ,  $V_{bc}$ ,  $V_{ba}$ ,  $V_{ca}$ , and  $V_{cb}$  are derived from a detector circuit. The width of the pulses is set to a constant value  $60^\circ$ . These pulses are detected through the input voltage from line to line and serve as input signals for the multiplexer/demultiplexer circuit (FPGA Altera). The PWM signals  $S_{11} - S_{33}$  are produced by the multiplexer/demultiplexer circuit (FPGA Altera). The modulation index allows for variation of the output voltage, and the frequency can be modified by altering the pulse-width modulation signals  $g_1 - g_6$ . Figure 3 illustrates these signals. The output voltage  $V_{OAB}$  is produced by multiplying the pulse-width modulation signals  $S_{11} - S_{33}$  with the input voltage signals. The results presented in Figure 3 demonstrate that the output voltage spectrum aligns well with both theoretical and experimental findings.

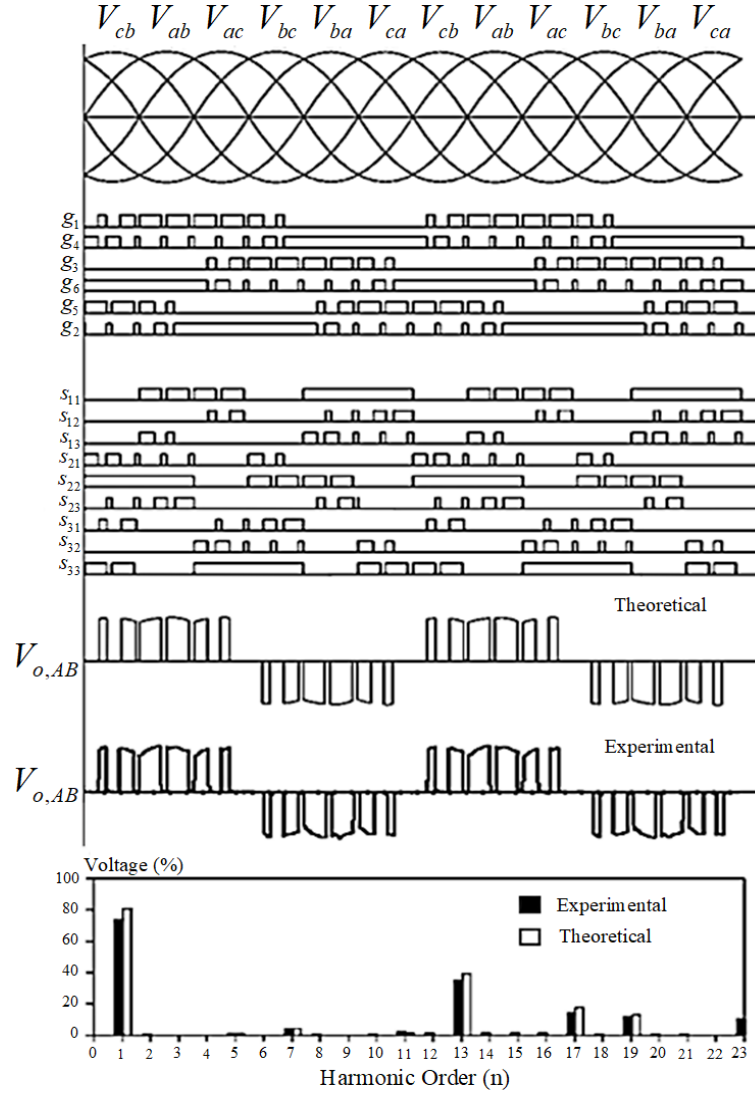


Figure 3. The output pulse-width modulation signals, pulse-width modulation voltage, and harmonic spectrum at an output frequency of 50 Hz, with a modulation index of 0.8 and a switching frequency ( $f_s$ ) of 0.6 kHz

### 3. A PRINCIPLE OF THE PWM GENERATION FROM THE OUTPUT VOLTAGE SIGNALS [31]

The pulse-width modulation generation is initially used to design the output voltage waveforms. This design process starts with the three-phase line-to-line input voltage waveforms of the power supply. The details of generating the output voltage waveform are as follows: The three-phase line-to-line input voltage waveforms are divided into six intervals, each spanning 60 degrees. Each interval contains two pulses, as illustrated in Figure 4. The ratios of the pulse widths are given by (9).

$$X1MT: (1 - X1)MT: MT: MT: (1 - X1)MT: X1MT \quad (9)$$

Where,  $X1$  is a pulse-width ratio of pulse-width modulation pulses,  $M$  is a modulation index (0 to 1),  $T$  is  $\frac{\pi}{m}$  (where  $m$  represents the quantity of pulses in each  $\frac{1}{2}$  cycle of the output frequency).

The output voltages of this converter can be illustrated mathematically by the Fourier series form in (9).

$$v_{AB}(\omega_o t) = \sum_{n=1}^{\infty} [a_n \cos n \omega_o t + b_n \sin n \omega_o t] \quad (10)$$

The coefficients of Fourier series form can be calculated by (11) and (12).

$$a_n = \frac{2}{T} \int_0^T f(\omega_o t) \cos n \omega_o t d(\omega_o t) \quad (11)$$

$$b_n = \frac{2}{T} \int_0^T f(\omega_o t) \sin n \omega_o t d(\omega_o t) \quad (12)$$

The harmonic spectrum of the output voltage at an output frequency of 50 Hz with a modulation index of 0.8 can be shown in Figure 3. In Figure 5, the output line voltage waveforms are shown at a modulation index of 0.8 and a frequency of 50 Hz. These waveforms are generated from the three-phase input voltages supplied through the three-phase matrix converter for the connected loads. These output waveforms can be designed by (8).

Afterward, the pulse-width modulation gating signal patterns  $g_1 - g_6$  are designed based on the input voltage from the supply. Each interval of the supply voltage is used to generate the pulse-width modulation gating signal patterns, as shown in Figure 6. Additionally, the pulse-width modulation signals  $S_{11} - S_{33}$  for the bidirectional switches are generated using (13). These signals utilize the supply voltages  $V_{ab}$ ,  $V_{ac}$ ,  $V_{bc}$ ,  $V_{ba}$ ,  $V_{ca}$ , and  $V_{cb}$ , for the control signals. The pulse-width modulation signals  $S_{11} - S_{33}$  are illustrated in Figure 3. The output voltage waveform contains harmonics, which can be reduced using this PWM method. The harmonic order can be determined by  $h = 6n \pm 1 : n = 1, 2, 3, \dots$  ( $h$  = harmonic order for the reducing).

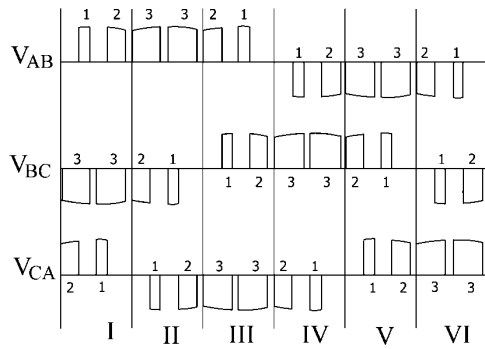


Figure 4. The 6-pulse three-phase output voltage as the design

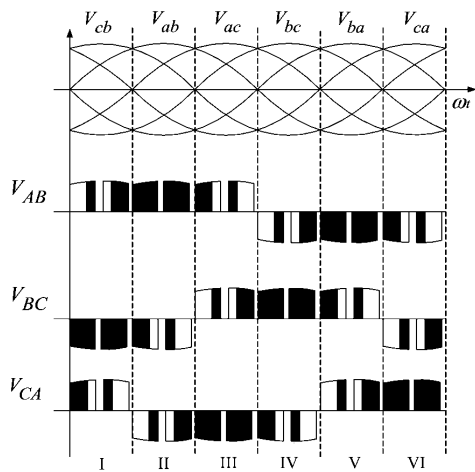


Figure 5. A comparison of the 6-pulse three-phase output voltage with the three-phase input voltage at  $M = 0.8$  and  $f = 50$  Hz

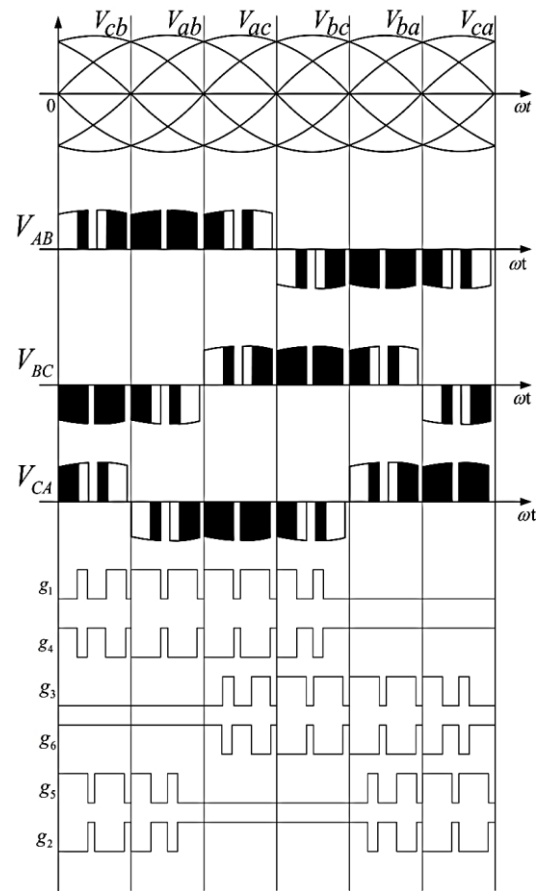


Figure 6. The pulse-width modulation gating signal pattern ( $g_1 - g_6$ ) for 6-pulse three-phase output voltage at  $M = 0.8$ ,  $f = 50$  Hz

#### 4. THE THREE-PHASE PWM MATRIX CONVERTER DESIGN

The overall system of the three-phase pulse-width modulation matrix converter can be seen in Figure 1. It comprises a microprocessor, a voltage detector circuit, an interrupt circuit, and a MUX/DMUX circuit. These various parts have the chance to be explained as (13).

$$\begin{aligned} S_{11} &= (V_{ab} + V_{ac})g_1 + (V_{ba} + V_{ca})g_4 \\ S_{12} &= (V_{ab} + V_{ac})g_3 + (V_{ba} + V_{ca})g_6 \end{aligned}$$

$$\begin{aligned}
S_{13} &= (V_{ab} + V_{ac})g_5 + (V_{ba} + V_{ca})g_2 \\
S_{21} &= (V_{bc} + V_{ba})g_1 + (V_{cb} + V_{ab})g_4 \\
S_{22} &= (V_{bc} + V_{ba})g_3 + (V_{cb} + V_{ab})g_6 \\
S_{23} &= (V_{bc} + V_{ba})g_5 + (V_{cb} + V_{ab})g_2 \\
S_{31} &= (V_{cb} + V_{ab})g_1 + (V_{ac} + V_{bc})g_4 \\
S_{32} &= (V_{cb} + V_{ab})g_3 + (V_{ac} + V_{bc})g_6 \\
S_{33} &= (V_{cb} + V_{ab})g_5 + (V_{ac} + V_{bc})g_2
\end{aligned} \tag{13}$$

#### 4.1. The PWM generation

This component is responsible for generating the pulse-width modulation signals  $g_1 - g_6$  used by the MUX/DMUX circuit. The signals are produced by a dsPIC30F2010 microprocessor and are synchronized with the source voltage through the interrupt signal. These pulse-width modulation signals have modulation index values of 0.2 to 0.8.

#### 4.2. The interrupt circuit

This component generates the signal of an interrupt for the dsPIC30F2010 microprocessor. The pulse-width modulation signals are aligned with this point where the supply voltage crosses zero. The non-maskable interrupt is connected to an interrupt-specific connector of the dsPIC30F2010 microprocessor. This interrupt signal is generated by the NE555 monostable circuit, as illustrated in Figure 7.

#### 4.3. Voltage detector circuit

The circuit produces these 6-square-waves needed for the MUX/DMUX circuit, where a signal has a breadth of about an angle of sixty degrees, and there are six signals. These square waves are produced by comparator circuits using the supply voltage. This process is depicted in Figure 8. All signals control the PWM signal in the MUX/DMUX circuit, which is connected to the bi-directional switches in the main circuit.

#### 4.4. Multiplexer/De-multiplexer circuit

The aim of the circuit is to generate PWM signals  $S_{11} - S_{33}$  for controlling the 9 bi-directional switches. These signals are generated by the voltage detector circuit and consist of  $V_{ab}$ ,  $V_{ac}$ ,  $V_{bc}$ ,  $V_{ba}$ ,  $V_{ca}$ , and  $V_{cb}$ . The microprocessor produces PWM signals  $g_1 - g_6$ , which control the bidirectional switches as described in Table 1, in accordance with (9). This equation is implemented through the FPGA chip (FPGA Altera), which is implemented to manage the 9 bi-directional switches in the main power converter circuit.

Table 1. The dealings with the pulse-width modulation signals, the source voltages, and the 9 bi-directional switches and their signals

PWM signals	Input voltages (line-to-line voltages)					
	$V_{cb}$	$V_{ab}$	$V_{ac}$	$V_{bc}$	$V_{ba}$	$V_{ca}$
$g_1$	$S_{31}$	$S_{11}$	$S_{11}$	$S_{21}$	$S_{21}$	$S_{31}$
$g_4$	$S_{21}$	$S_{21}$	$S_{31}$	$S_{31}$	$S_{11}$	$S_{11}$
$g_3$	$S_{32}$	$S_{12}$	$S_{12}$	$S_{22}$	$S_{22}$	$S_{32}$
$g_6$	$S_{22}$	$S_{22}$	$S_{32}$	$S_{32}$	$S_{12}$	$S_{12}$
$g_5$	$S_{33}$	$S_{13}$	$S_{13}$	$S_{23}$	$S_{23}$	$S_{33}$
$g_2$	$S_{23}$	$S_{23}$	$S_{33}$	$S_{33}$	$S_{13}$	$S_{13}$

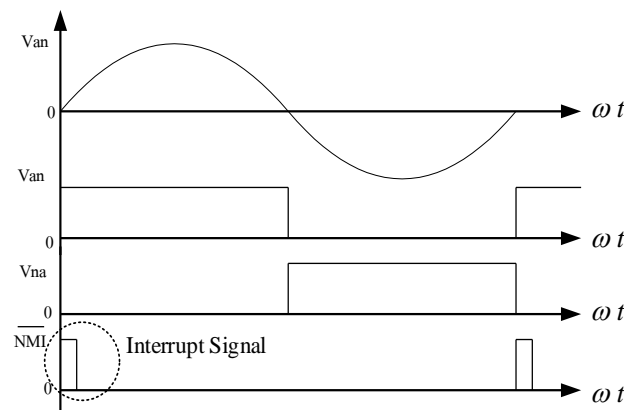


Figure 7. The monostable and interrupt signal

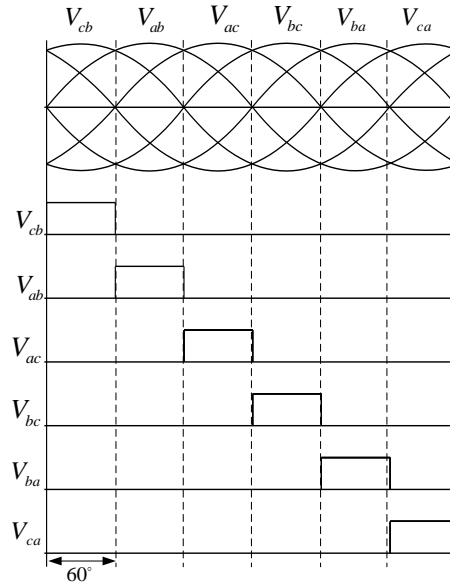


Figure 8. The voltage detector signals

## 5. ANALYSIS OF THE CONVERTER CIRCUIT

The three-phase PWM matrix converter is structured with nine bidirectional switches, as illustrated in Figure 1. Each switch is composed of a single IGBT and four power diodes arranged in a bridge configuration. These switches convert a constant amplitude and frequency three-phase input voltage into a three-phase output voltage with adjustable frequency and amplitude. The modulation index regulates both the amplitude and frequency, while the pulse-width modulation signal frequency produced by the dsPIC30F2010 processor also influences the control. Figure 9 displays the various operating conditions of the matrix converter (3MC), revealing that these operations can be categorized into six fundamental types:

- i) Status 1: This mode sees  $S_{21}, S_{22}, S_{23}, S_{31}, S_{32}$ , and  $S_{33}$  all activated, while  $V_{cb}$  represents the voltage source. The following sequence of events shows the generation of output line voltages, opening with a current move from  $V_c$ , going via  $S_{31}$ , and reaching  $Z_A$  whereupon the current subsequently proceeds, returning to the source ( $V_b$ ) through  $S_{22}$ . This creates the resulting voltage across the load given by  $V_{AB}$ . Simultaneously, this current moves from the source ( $V_c$ ), going via  $S_{32}$ , and reaching  $Z_B$  whereupon the current returns to the source ( $V_b$ ) through  $S_{23}$ . The resultant voltage across the load in this case is given by  $V_{BC}$ . Ultimately, the current flow runs from the source ( $V_c$ ) going via  $S_{33}$ , and reaching  $Z_C$ . The current then returns to the source ( $V_b$ ) through  $S_{21}$  with the resulting voltage across the load given by  $V_{CA}$ .
- ii) Status 2: This mode sees  $S_{11}, S_{12}, S_{13}, S_{21}, S_{22}$ , and  $S_{23}$  all activated.  $V_{ab}$  represents the voltage source. The following sequence of events shows the output line voltage synthesis. Initially, the flow of current comes from the source ( $V_a$ ), going via  $S_{11}$ , and reaching  $Z_A$ . The current then moves return to the source ( $V_b$ ) through  $S_{22}$ . The resulting voltage is thus given by  $V_{AB}$ . Simultaneously, the current moves outward from the source ( $V_a$ ) going via  $S_{12}$  and reaching  $Z_B$ , before flowing return to the source ( $V_b$ ) through  $S_{23}$ , while  $V_{BC}$  denotes the resulting voltage across the load. The final load voltage is  $V_{CA}$ . The current then continues to flow from the source ( $V_a$ ) going via  $S_{13}$  reaching  $Z_C$ , before returning to the source ( $V_b$ ) through  $S_{21}$ .
- iii) Status 3: This mode sees  $S_{11}, S_{12}, S_{13}, S_{31}, S_{32}$ , and  $S_{33}$  all activated, while  $V_{ac}$  shows the voltage source. The current then proceeds from the source ( $V_a$ ) via  $S_{11}$  to  $Z_A$  before returning to the source ( $V_c$ ) through  $S_{32}$ .  $V_{AB}$  is the load voltage. In the case of the voltage at the load being  $V_{BC}$ , the current then flows from the source ( $V_a$ ) via  $S_{12}$  to  $Z_B$ , and then returns to the source ( $V_c$ ) through  $S_{33}$ . Eventually, the current starts at the source ( $V_a$ ), flows via  $S_{13}$  to  $Z_C$ , and returns to the source ( $V_c$ ) via  $S_{31}$ .  $V_{CA}$  is the resulting voltage across the load.
- iv) Status 4: This mode sees  $S_{21}, S_{22}, S_{23}, S_{31}, S_{32}$ , and  $S_{33}$  all activated. The supply voltage is given by  $V_{bc}$ . The current starts with the source ( $V_b$ ) and flows via  $S_{21}, Z_A$  and  $S_{32}$  to the source ( $V_c$ ), while the resulting voltage across the load is given by  $V_{AB}$ . Simultaneously, the current flow runs from the source ( $V_b$ ) along  $S_{22}$  to  $Z_B$  before returning to the source ( $V_c$ ) along  $S_{33}$ . In this scenario, the resulting voltage across the load is influenced by  $V_{BC}$ . Ultimately, the current flow runs from the source ( $V_b$ ) throughout  $S_{23}$  to  $Z_C$  and subsequently returning to the source ( $V_c$ ) throughout  $S_{31}$  while the resulting voltage across the load is indicated by  $V_{CA}$ .



- v) Status 5: This mode sees  $S_{11}, S_{12}, S_{13}, S_{21}, S_{22}$ , and  $S_{23}$  all activated while  $V_{ba}$  denotes the input line voltage. The following sequence outlines the process of generating output line voltages, starting with the current flowing from the source ( $V_b$ ) throughout  $S_{11}$  to  $Z_A$ . The current then moves backward to the source ( $V_a$ ) throughout  $S_{22}$  while the resulting load voltage is  $V_{AB}$ . Simultaneously, the current moves from the supply ( $V_b$ ) throughout  $S_{12}$  to  $Z_B$  before flowing return to the source ( $V_a$ ) throughout  $S_{23}$ . The resulting voltage across the load is given by  $V_{BC}$ . At the end, the voltage at the load is  $V_{CA}$ . The current flow then runs from the supply ( $V_b$ ) along  $S_{13}$  to  $Z_C$  prior to flowing, return to the source ( $V_a$ ) throughout  $S_{21}$ .
- vi) Status 6: This mode sees  $S_{11}, S_{12}, S_{13}, S_{31}, S_{32}$ , and  $S_{33}$  all activated with an input voltage given by  $V_{ca}$ . In this scenario, the current runs from the  $V_c$  along  $S_{31}$  to  $Z_A$ . The current then moves, returning to the source ( $V_a$ ) through  $S_{12}$  while  $V_{AB}$  indicates the resulting voltage across the load. If the voltage at load is given by  $V_{BC}$ , the current will flow from the source ( $V_c$ ) via  $S_{32}$  to  $Z_B$  before flowing return to the source ( $V_a$ ) through  $S_{13}$ . Ultimately, the current flow runs from the source ( $V_c$ ) throughout  $S_{33}$  to  $Z_C$  before flowing return to the source ( $V_a$ ) through  $S_{11}$ . In this scenario, the resulting voltage across the lo, is  $V_{CA}$  and the operational cycle is repeated.

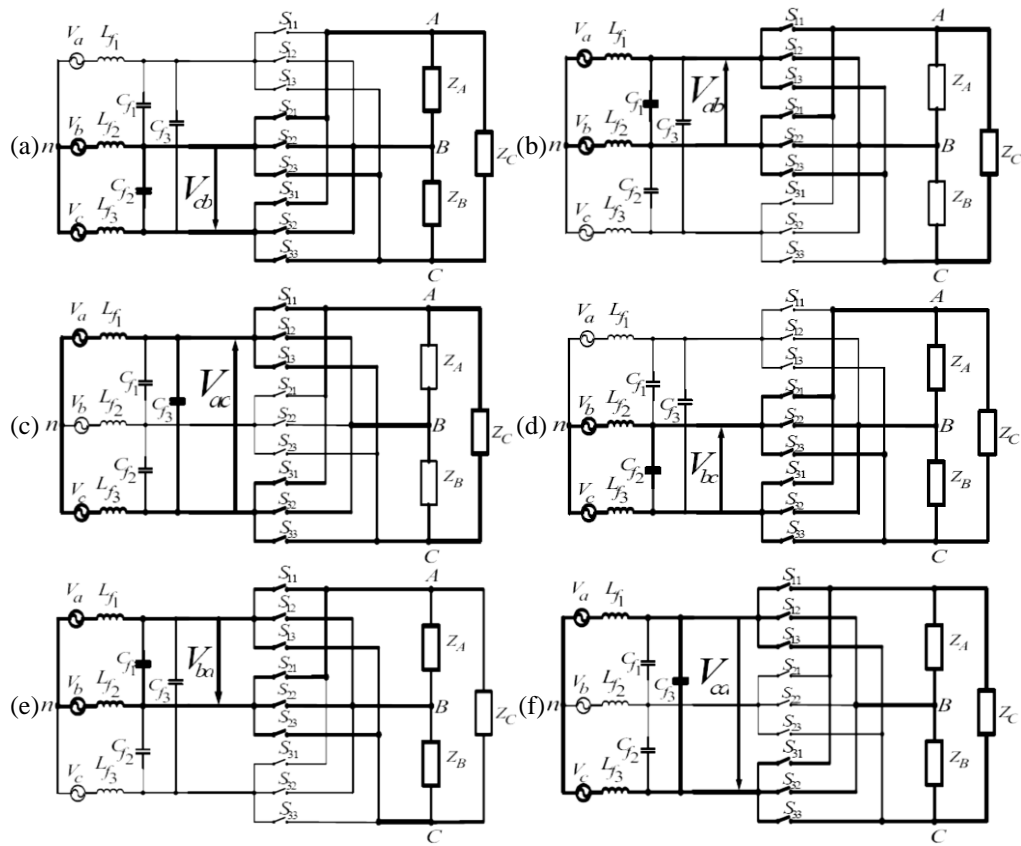


Figure 9. The principal operating modes: (a) status 1 ( $V_{cb}$ ), (b) status 2 ( $V_{ab}$ ), (c) status 3 ( $V_{ac}$ ), (d) status 4 ( $V_{bc} V_{bc}$ ), (e) status 5 ( $V_{ba}$ ), and (f) status 6 ( $V_{ca}$ )

## 6. RESULTS OF EXPERIMENTAL AND DISCUSSION

In this study, the matrix converter was developed, implemented, and tested in a laboratory setting. The pulse-width modulation signals featured six pulses per  $\frac{1}{2}$  cycle, with modulation indices of 0.2 to 0.8, and primary frequencies of 25 Hz to 100 Hz. Figures 10 and 11 present the output voltage waveforms and harmonic spectra for six pulses per  $\frac{1}{2}$  cycle, emphasizing the changes in frequencies, modulation indices ( $M$ ), and frequencies of the switches  $f_s$ . These results from both practical and theoretical cases are in good agreement. Figure 12 depicts the correlation between the output voltage and the fundamental frequency ratio for each modulation index ( $M$ ), and the experimental setup can be seen in Figure 13. Additionally, this data was utilized to regulate the speed of the induction motor using the V/f method for the speed control in future work.

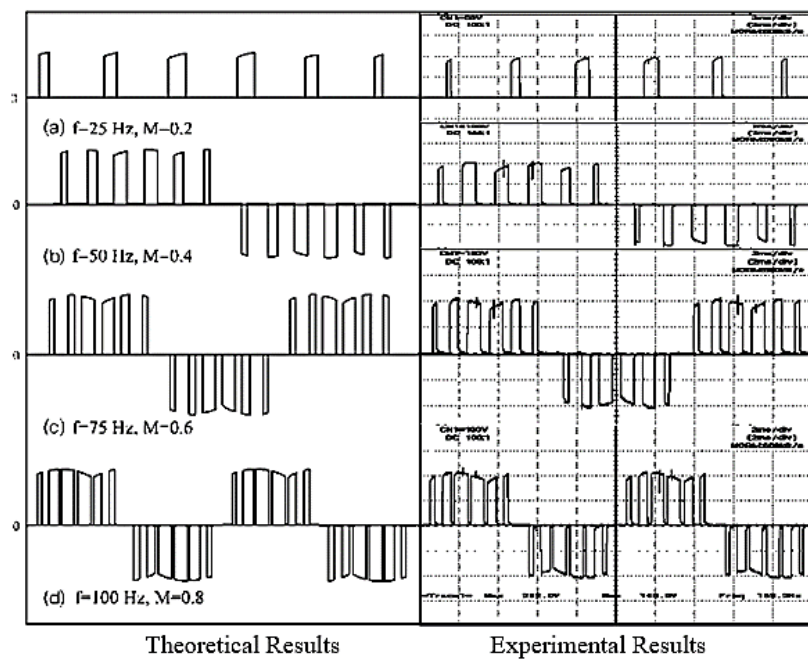


Figure 10. Output voltage waveforms in the theoretical and practical cases at various frequencies and various modulation indices ( $M$ )

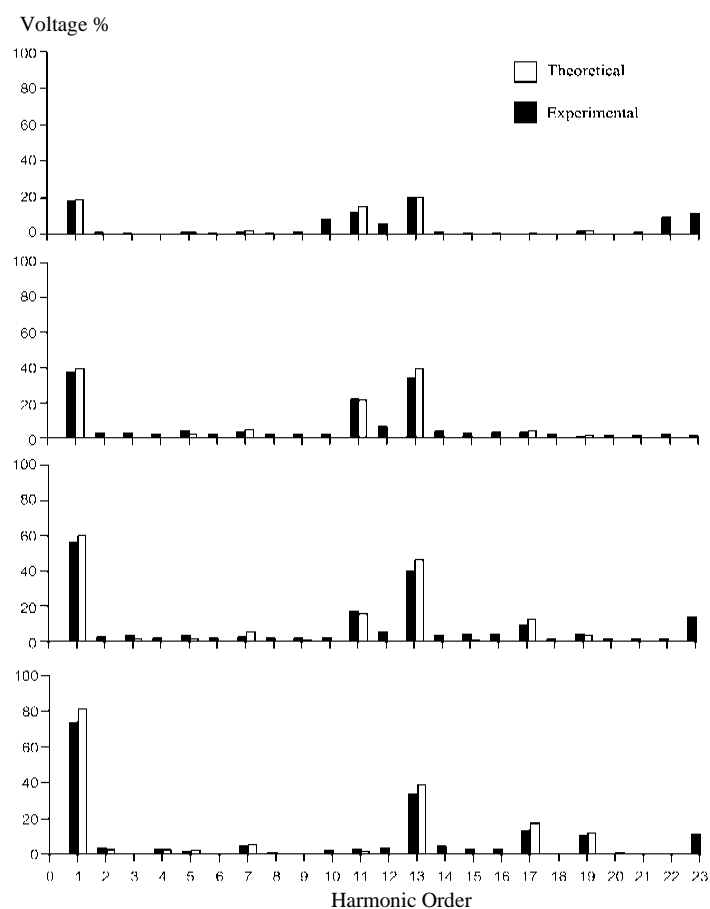


Figure 11. The harmonic spectra are showing the theoretical and practical output voltage waveforms for varying frequencies and modulation indices ( $M$ ) from Figure 10

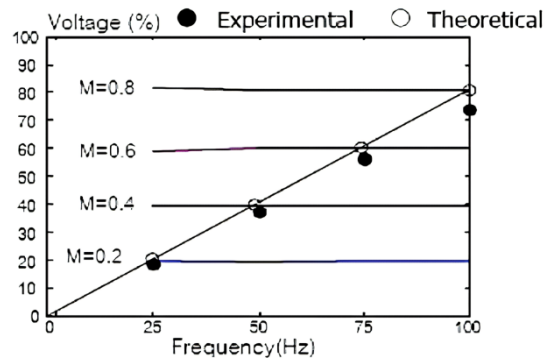


Figure 12. Connection between load voltage and fundamental frequency for the V/f control system



Figure 13. Overall, of the experimental testing in the laboratory

## 7. CONCLUSION

This study confirms the feasibility of creating and building a prototype for a three-phase PWM matrix converter. The matrix converter's principle can be mathematically represented by equations, which are depicted through graphical waveforms. These waveforms can be generated through computer simulations, which can then be compared with experimental outcomes for voltage waveforms and harmonic spectra. The findings are shown in the results. The system was tested with six pulses per half-cycle and modulation index values of 0.2, 0.4, 0.6, and 0.8. The converter load was passive loads (RL Loads), and the waveforms demonstrate that the results of the experiment closely align with the simulation results. The harmonic content of the output voltage can be calculated and measured for various applications. These output voltages and fundamental frequencies are obtained from experimental data and calculations as linear results. This indicates that the findings are applicable to three-phase IM drive systems using V/f control. The V/f control implementation for the induction motor drive is discussed in the next paper. All data verify that the PWM technique is effective with controlled by the direct three-phase matrix converter. These results verify the performance and capability of the proposed converter, demonstrating its applicability in various tasks. In future work, this matrix converter will drive an induction motor using the V/f method for both open-loop and closed-loop speed control.

## ACKNOWLEDGEMENTS AND FUNDING INFORMATION

The author thanks the Thailand Science Research and Innovation (TSRI), and Fund of Rajamangala University of Technology Rattanakosin. In most cases, sponsor and financial support acknowledgments. Funding was also received from the Thailand Science Research and Innovation (TSRI) and Fund of Rajamangala University of Technology Rattanakosin 2023, (No. 181481).

## AUTHOR CONTRIBUTIONS STATEMENT

This journal uses the Contributor Roles Taxonomy (CRediT) to recognize individual author contributions, reduce authorship disputes, and facilitate collaboration.

Name of Author	C	M	So	Va	Fo	I	R	D	O	E	Vi	Su	P	Fu
Prasopchok	✓	✓	✓	✓	✓	✓	✓	✓	✓	✓	✓	✓	✓	✓
Hothongkham														
Sataporn Suathed	✓	✓	✓		✓	✓		✓	✓	✓	✓		✓	✓
Anuchit Aurairat	✓	✓		✓	✓	✓			✓	✓	✓	✓	✓	✓

C : Conceptualization

M : Methodology

So : Software

Va : Validation

Fo : Formal analysis

I : Investigation

R : Resources

D : Data Curation

O : Writing - Original Draft

E : Writing - Review & Editing

Vi : Visualization

Su : Supervision

P : Project administration

Fu : Funding acquisition

## CONFLICT OF INTEREST STATEMENT

Authors state no conflict of interest.

## DATA AVAILABILITY

The data that support the findings of this study are available from the corresponding author, [PH], upon reasonable request.




## REFERENCES

- [1] L. Gyugyi and B. R. Pelly, *Static power frequency changers: theory, performance, and application*. 1976. [Online]. Available: <http://books.google.com/books?id=MPZSAAAAMAAJ&pgis=1>
- [2] B. R. Pelly, "Thyristor phase-controlled converters and cycloconverters," 1971.
- [3] A. Alesina and M. Venturini, "Solid-state power conversion: A fourier analysis approach to generalized transformer synthesis," *IEEE Transactions on Circuits and Systems*, vol. 28, no. 4, pp. 319–330, Apr. 1981, doi: 10.1109/TCS.1981.1084993.
- [4] P. D. Ziogas, S. I. Khan, and M. H. Rashid, "Some improved forced commutated cycloconverter structures," *IEEE Transactions on Industry Applications*, vol. IA-21, no. 5, pp. 1242–1253, Sep. 1985, doi: 10.1109/TIA.1985.349549.
- [5] A. Alesina and M. G. B. Venturini, "Analysis and design of optimum-amplitude nine-switch direct AC–AC converters," *IEEE Transactions on Power Electronics*, vol. 4, no. 1, pp. 101–112, 1989, doi: 10.1109/63.21879.
- [6] P. D. Ziogas, S. I. Khan, and M. H. Rashid, "Analysis and design of forced commutated cycloconverter structures with improved transfer characteristics," *IEEE transactions on industrial electronics and control instrumentation*, vol. IE-33, no. 3, pp. 271–280, 1986, doi: 10.1109/tie.1986.350233.
- [7] S. Ratanapanachote, H. J. Cha, and P. N. Enjeti, "A digitally controlled switch mode power supply based on matrix converter," in *2004 IEEE 35th Annual Power Electronics Specialists Conference (IEEE Cat. No.04CH37551)*, IEEE, 2004, pp. 2237–2243. doi: 10.1109/PESC.2004.1355468.
- [8] E. Erdem, Y. Tatar, and S. Sünter, "Modeling and simulation of matrix converter using space vector control algorithm," *EUROCON 2005 - The International Conference on Computer as a Tool*, vol. II, pp. 1228–1231, 2005, doi: 10.1109/eurcon.2005.1630177.
- [9] K. Spiteri, C. S. Staines, and M. Apap, "A three phase to three phase bidirectional power matrix converter," *2008 3rd International Symposium on Communications, Control, and Signal Processing, ISCCSP 2008*, pp. 1404–1408, 2008, doi: 10.1109/ISCCSP.2008.4537446.
- [10] N. P. R. Iyer, "Carrier based modulation technique for three phase matrix converters - state of the art progress," *Proceedings - 2010 IEEE Region 8 International Conference on Computational Technologies in Electrical and Electronics Engineering, SIBIRCON-2010*, pp. 659–664, 2010, doi: 10.1109/SIBIRCON.2010.5555147.
- [11] A. A. Heris, M. Sadeghi, and E. Babaei, "A new topology for the three-phase to three-phase cycloconverters," *2011 2nd Power Electronics, Drive Systems and Technologies Conference, PEDSTC 2011*, pp. 489–494, 2011, doi: 10.1109/PEDSTC.2011.5742468.
- [12] P. Hothongkham, "Theoretical and practical analysis of 6-pulse three-phase PWM AC-AC matrix converter," *ECTI-CON 2011 - 8th Electrical Engineering/ Electronics, Computer, Telecommunications and Information Technology (ECTI) Association of Thailand - Conference 2011*, pp. 739–743, 2011, doi: 10.1109/ECTICON.2011.5947946.
- [13] P. Hothongkham, S. Kongkachat, and N. Thodsaporn, "Synthesis and design of three-phase PWM AC-AC matrix converter," *IEEE Region 10 Annual International Conference, Proceedings/TENCON*, pp. 1020–1024, 2011, doi: 10.1109/TENCON.2011.6129265.
- [14] A. Iqbal and H. Abu-Rub, "Space vector PWM technique for a three-to-five-phase matrix converter," *IEEE Transactions on Industry Applications*, vol. 48, no. 2, pp. 697–707, Mar. 2012, doi: 10.1109/TIA.2011.2181469.
- [15] T. D. Nguyen and H. Lee, "Dual three-phase indirect matrix converter with carrier-based PWM method," *IEEE Transactions on Power Electronics*, vol. 29, no. 2, pp. 569–581, 2014, doi: 10.1109/TPEL.2013.2255067.
- [16] S. M. Ahmed, H. Abu-Rub, Z. Salam, and A. Kouzou, "Space vector PWM technique for a novel three-to-seven phase matrix converter," in *IECON 2013 - 39th Annual Conference of the IEEE Industrial Electronics Society*, IEEE, Nov. 2013, pp. 4949–4954. doi: 10.1109/IECON.2013.6699936.
- [17] N. Rizoug, B. Francois, O. Bouhali, and T. Mesbahi, "Modeling and control of the three-phase NPC multilevel converter using an equivalent matrix structure," in *7th IET International Conference on Power Electronics, Machines and Drives (PEMD 2014)*, Institution of Engineering and Technology, 2014, pp. 0054–0054. doi: 10.1049/cp.2014.0264.
- [18] F. E. Rodarte-Gutierrez, I. Araujo-Vargas, and J. R. Hernandez, "FPGA Implementation of a three-phase PLL and a space vector modulator of a matrix converter for future electric vehicles," in *2015 IEEE Vehicle Power and Propulsion Conference (VPPC)*, IEEE, Oct. 2015, pp. 1–8. doi: 10.1109/VPPC.2015.7352949.
- [19] Sandeep J., Ashok S., and R. Ramchand, "Carrier based space vector modulation for matrix converters," in *2016 IEEE 1st International Conference on Power Electronics, Intelligent Control and Energy Systems (ICPEICES)*, IEEE, Jul. 2016, pp. 1–6. doi: 10.1109/ICPEICES.2016.7853062.
- [20] L. Schrittwieser, P. Cortes, L. Fassler, D. Bortis, and J. W. Kolar, "Modulation and control of a three-phase phase-modular isolated matrix-type PFC rectifier," *IEEE Transactions on Power Electronics*, vol. 33, no. 6, pp. 4703–4715, Jun. 2018, doi: 10.1109/TPEL.2017.2726342.
- [21] P. B. Shinde and T. N. Date, "Pulse width modulation control of 3 phase AC-AC matrix converter," in *2017 International Conference on Computing Methodologies and Communication (ICCMC)*, IEEE, Jul. 2017, pp. 992–997. doi: 10.1109/ICCMC.2017.8282618.
- [22] J. Kaniewski, "Three-phase power flow controller based on bipolar AC/ AC converter with matrix choppers," in *2018 International Symposium on Power Electronics, Electrical Drives, Automation and Motion (SPEEDAM)*, IEEE, Jun. 2018, pp. 709–715. doi: 10.1109/SPEEDAM.2018.8445200.
- [23] M. Moghaddami and A. Sarwat, "A three-phase AC-AC matrix converter with simplified bidirectional power control for inductive power transfer systems," in *2018 IEEE Transportation Electrification Conference and Expo (ITEC)*, IEEE, Jun. 2018, pp. 380–384. doi: 10.1109/ITEC.2018.8450244.
- [24] S. M. Dabour, I. Masoud, and E. M. Rashad, "Carrier-based PWM technique for a new six-to-three-phase multilevel matrix converter for wind-energy conversion systems," in *2019 IEEE Conference on Power Electronics and Renewable Energy (CPERE)*, IEEE, Oct. 2019, pp. 412–417. doi: 10.1109/CPERE45374.2019.8980202.




- [25] W. Xiong, T. Liu, Y. Sun, M. Su, P. Zeng, and H. Dan, "Modulation strategies based on mathematical construction method for three-to-five-phase matrix converters," in *2020 IEEE 9th International Power Electronics and Motion Control Conference (IPEMC2020-ECCE Asia)*, IEEE, Nov. 2020, pp. 2452–2457. doi: 10.1109/IPEMC-ECCEAsia48364.2020.9368089.
- [26] S. Wu, Y. Wei, X. Guo, Z. Zhang, and P. Zhang, "A new modulation strategy to improve the performance of bidirectional isolated AC-DC matrix converter," in *2022 IEEE International Power Electronics and Application Conference and Exposition (PEAC)*, IEEE, Nov. 2022, pp. 307–310. doi: 10.1109/PEAC56338.2022.9959092.
- [27] H. M. Langa and K. Moloi, "Modelling a three-phase to single-phase AC-AC matrix converter," in *2024 1st International Conference on Trends in Engineering Systems and Technologies (ICTEST)*, IEEE, Apr. 2024, pp. 1–6. doi: 10.1109/ICTEST60614.2024.10576189.
- [28] Y. Wei, F. Wu, S. Wu, and H. Liu, "Improved modulation strategy for three-phase matrix converter-based WPT system," *IEEE Transactions on Transportation Electrification*, vol. 10, no. 2, pp. 3396–3406, Jun. 2024, doi: 10.1109/TTE.2023.3302299.
- [29] H. Sun, T. Zhang, and J. Jiang, "Zero-vector-reconfiguration based SVPWM technique for ZVZCS and voltage spike suppression high-frequency link three-phase AC-DC converter," *IEEE Transactions on Power Electronics*, vol. 39, no. 5, pp. 5536–5546, May 2024, doi: 10.1109/TPEL.2024.3368345.
- [30] P. Hothongkham and S. Suathed, "Simulation of three-phase PWM AC-AC matrix converter without the DC-link testing with the passive loads and without input filter," in *2022 19th International Conference on Electrical Engineering/Electronics, Computer, Telecommunications and Information Technology (ECTI-CON)*, IEEE, May 2022, pp. 1–4. doi: 10.1109/ECTI-CON54298.2022.9795562.
- [31] P. Viriya, H. Kubota, and K. Matsuse, "New PWM-controlled GTO converter," *IEEE Transactions on Power Electronics*, vol. 2, no. 4, pp. 373–381, 1987, doi: 10.1109/TPEL.1987.4307874.

## BIOGRAPHIES OF AUTHORS






**Prasopchok Hothongkham**    is a lecturer in the Electrical Engineering Department at Rajamangala University of Technology Rattanakosin, Thailand, since 2011 and was been lecturer in the Electrical Engineering Department at SIAM University, Thailand, from 1997 to 2011. He received his B. Eng., degree in Electrical Engineering from SIAM University, Thailand, in 1995. And received his M.Eng. and D.Eng. degrees in Electrical Engineering from King Mongkut's Institute of Technology, Ladkrabang, Thailand, in 2002 and 2010, respectively. He became an assistant professor in 2013, an associate professor in 2024. His research interests include power electronics and applications, motor drives, and renewable energy. He can be contacted at email: prasopchok.hot@rmutr.ac.th.



**Sataporn Suathed**    has been a lecturer in the Mechatronics Engineering Department at Rajamangala University of Technology Rattanakosin, Thailand, since 2013. He received a B.Eng. degree in Electrical Engineering from Pathumthani University and an M.Eng. degree in Control System Engineering from King Mongkut's Institute of Technology, Ladkrabang, Thailand. He was promoted to assistant professor in 2023. His research interests include power electronics, motor drives, control systems, and embedded systems. He can be contacted at email: sataporn.sua@rmutr.ac.th.



**Anuchit Aurairat**    is a lecturer in the Department of Electrical Engineering Technology at the Rajamangala University of Technology Rattanakosin, Thailand. He received his B.Eng. in Electrical Engineering from the Rajamangala University of Technology Thanyaburi, M.S. in Electrical Power Engineering from the King Mongkut's University of Technology North Bangkok, and D.Eng. degrees in Electrical Engineering from the Rajamangala University of Technology Thanyaburi. His research interests include power electronics, motor drives, renewable energy, FPGA applications, embedded systems, artificial intelligence, intelligent control, and digital libraries. He can be contacted at email: anuchit.aur@rmutr.ac.th.